Sam Liao*, Brendan Langfield, Nikola Ristovski, Christina Theodoropoulos, Jake Hardt, Keith A. Blackwood, Soniya D. Yambem, Shaun D. Gregory, Maria A. Woodruff and Sean Powell

Effect of humidity on melt electrospun polycaprolactone scaffolds

DOI 10.1515/bnm-2016-0009
Received May 24, 2016; accepted August 12, 2016

Abstract: Direct write melt electrospinning is an additive manufacturing technique used to produce 3D polymer scaffolds for tissue engineering applications. It is similar to conventional 3D printing by layering 2D patterns to build up an object, but uses a high-electric potential to draw out fibres into micron-scale diameters with great precision. Direct write melt electrospinning is related to a well-established fabrication technique, solution electrospinning, but extrudes a melted polymer in a controlled manner rather than a polymer solution. The effect of environmental conditions such as humidity has been extensively studied in the context of solution electrospinning; however, there is a lack of similar studies for direct write melt electrospinning. In this study, melt electrospun polycaprolactone scaffolds were produced with 90 degree cross-hatch architecture at three specific humidity [H_2O/air (g/kg)] levels, low (0.74 g/kg), standard (8.94 g/kg), and elevated (11.26 g/kg). Micro-computed tomography and scanning electron microscopic analysis was performed on the scaffolds to investigate the degree to which humidity affects inter-layer ordering, fibre diameter consistency, and fibre surface morphology. Results indicated that humidity does not play a significant role in affecting these scaffold parameters during fabrication within the levels investigated.

Keywords: biofabrication; fibres; humidity; melt electrospinning; polycaprolactone; polymers.

***Corresponding author: Sam Liao,** Queensland University of Technology (QUT), Institute of Health and Biomedical Innovation (IHBI), Kelvin Grove, QLD 4059, Australia; and Innovative Cardiovascular Engineering and Technology Laboratory (ICETLAB), Critical Care Research Group, The Prince Charles Hospital, Chermside, QLD 4032, Australia, E-mail: sam.liao@hdr.qut.edu.au
Brendan Langfield, Nikola Ristovski, Christina Theodoropoulos, Jake Hardt, Keith A. Blackwood, Soniya D. Yambem, Maria A. Woodruff and Sean Powell: Queensland University of Technology (QUT), Institute of Health and Biomedical Innovation (IHBI), Kelvin Grove, QLD 4059, Australia
Shaun D. Gregory: Innovative Cardiovascular Engineering and Technology Laboratory (ICETLAB), Critical Care Research Group, The Prince Charles Hospital, Chermside, QLD 4032, Australia; The University of Queensland, School of Medicine, St. Lucia, QLD 4072, Australia; and Griffith University, School of Engineering, Southport, QLD 4215, Australia

Introduction

Direct write melt electrospinning is an additive manufacturing technique used to fabricate polymer scaffolds with high precision. A molten polymer is extruded from a needle tip onto a collector plate in the presence of a high-electric potential. This potential acts on the polymer to draw out a fibre with micron-scale diameter (~20 μm) [1]. The collector plate is translated in the x, y and z axes to produce 2D patterns, which are layered to produce a 3D construct (see Figure 1). Melt electrospinning is related to solution electrospinning, a well-established method for producing fibre-based polymer scaffolds where the polymer is dissolved in a solvent which evaporates during deposition, producing fibres. The use of a polymer *melt* in place of a *solution* results in higher viscosity and consequently, higher degrees of control during the fabrication process. Both electrospinning techniques are highly suited for tissue engineering applications as they can produce 3D structures with significantly thinner fibres than other additive manufacturing techniques such as fused deposition modelling [2]. The resulting scaffolds have relatively higher surface area to volume ratios and excellent pore interconnectivity [3, 4]. Altering various parameters such as electric potential or stage translation allows customisation of scaffold characteristics. These include overall shape, fibre diameter, internal scaffold microarchitecture and pore size. Due to its wide use in tissue engineering, electrospinning has been extensively described in literature and detailed overviews can be found in Pham et al. [5] for solution electrospinning, and Brown et al. [6] for melt electrospinning.

Electrospinning is sensitive to environmental conditions such as temperature and humidity. This sensitivity

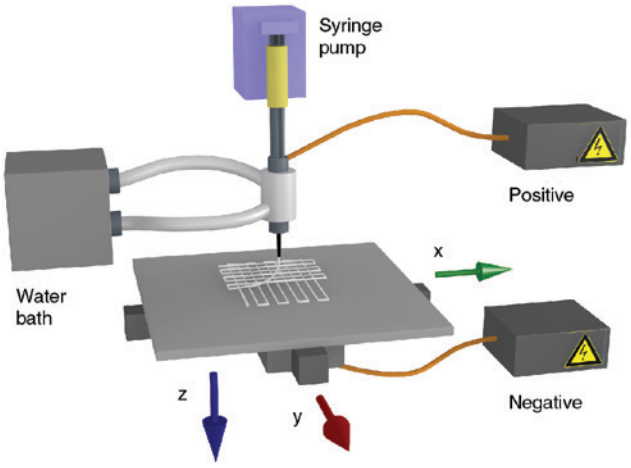

Figure 1: Schematic of the direct-write melt-electrospinning apparatus. The water bath is used to melt a PCL polymer which is extruded onto a moving collector plate via the syringe pump. 2D patterns are stacked to produce a 3D polymer construct. A positive and negative voltage is applied to the needle and collector, respectively, to draw out the polymer into a micron-diameter fibre.

has been well documented in several studies investigating the effect of humidity on solution electrospinning [7–14]. As the formation of fibres in solution electrospinning is through solvent evaporation following extrusion, the process is highly susceptible to the humidity [15]. To our knowledge, there are no quantitative studies investigating the effect of humidity on the process of melt electrospinning.

During solution electrospinning, Pelipenko et al. [7] reported that different polymers [poly(vinyl alcohol), poly(ethylene oxide), poly(vinyl alcohol)/hyaluronic acid and poly(ethylene oxide)/chitosan] presented variations in fibre size and morphology with changes in relative humidity (RH) between 4% and 70% RH. As RH decreased, an increase in fibre size was observed. Pelipenko et al. [7] controlled RH using silica gel and an ultrasonic humidifier. This increase in fibre size with decreasing RH was also observed by Medeiros et al. [11] with poly(vinyl alcohol) between 20% and 80% RH. However, when Medeiros et al. [11] used polystyrene, poly(vinyl chloride), poly(methyl methacrylate), and poly(lactic acid) an increase in fibre size was observed with increases in RH. Ogulata and Icoglu [8] found increases in fibre size with increasing RH when polyetherimide was investigated between 30% and 70% RH. As RH increased further, droplets started to form with poly(vinyl alcohol), poly(ethylene oxide), poly(vinyl alcohol)/hyaluronic acid, poly(ethylene oxide)/chitosan and polystyrene as evaporation rates lowered [7, 9, 10]. Yao et al. [16] reported that by electrospinning a hyaluronic acid solution above a critical RH value, which is dependent on solution concentration, dissolving of fibres at intersections and fused layer spreading was observed. Casper et al. [12] reported surface features started to appear when RH was increased above 30%, using polystyrene. Further increases in RH increased the number, diameter and distribution of pores Casper et al. [12]. In addition, Lu and Xia [10] and Nezarati et al. [13] found similar results where surface features appeared when RH was increased.

In addition to humidity, other parameters such as polymer solution concentration, flow rate, and tip to collector distance have been studied for both solution and melt electrospinning. The effect of the electric field on resultant scaffold structure has been studied [1, 17, 18]. In this paper, we investigated the effect of humidity on the melt electrospinning of polycaprolactone scaffolds at three different humidity levels: low (0.74 g/kg), standard (lab conditions) (8.94 g/kg), and elevated (11.26 g/kg).

Results

Mean and standard deviation of the order parameter and fibre diameter can be found in Table 1. Scaffold fibre morphology was observed to be similar between all groups, as seen in Figure 2. Images taken from an oblique angle to the scaffold (Figure 2B, E and H) showed stacking of fibres and some fibre fusing between layers, forming walled compartments with randomly distributed periodic wall breaks. Figure 2C, F and I showed no noticeable difference, as detectable by SEM, in fibre surface morphology between scaffolds produced at each humidity level.

The humidity system, controlled using an air saturator and drier, was able to achieve a minimum and maximum specific humidity level of 0.74 g/kg and 11.26 g/kg, respectively, as seen in Table 1. Scaffolds were made during the stabilised region, seen in Figure 3, for elevated and low humidity levels, after 3 h. Mean temperatures were 39.4 °C ± 0.2, 40 °C ± 1 and 36 °C ± 1 for low, standard and elevated humidity levels, respectively. This was equivalent

Table 1: Average order parameter and fibre diameter for three different environmental conditions.

	Specific humidity (g/kg)	Order parameter	Fibre diameter (µm)
Low	0.74 ± 0.01	1.10 ± 0.03	57 ± 7
Standard	8.94 ± 0.05	1.10 ± 0.04	47 ± 7
Elevated	11.26 ± 0.06	1.15 ± 0.10	53 ± 9

No significant difference was found between the groups. Significance defined by $p \leq 0.01$.

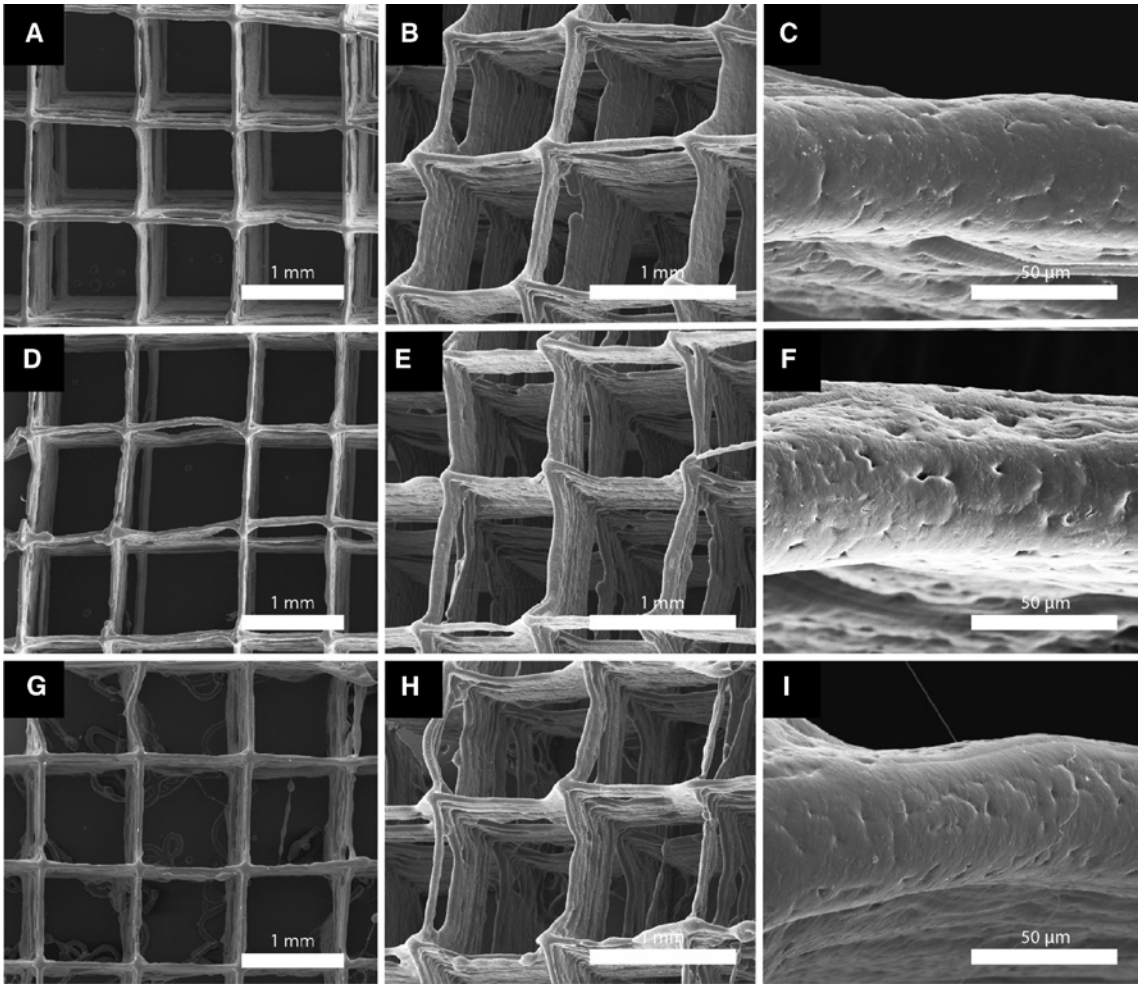

Figure 2: Representative SEM of each scaffold at different humidity levels. (A–C): Low humidity, (D–F): standard humidity, and (G–I): elevated humidity. No noticeable difference is seen within the imaging parameters of scaffold ordering, fibre diameter or fibre surface morphology across all groups.

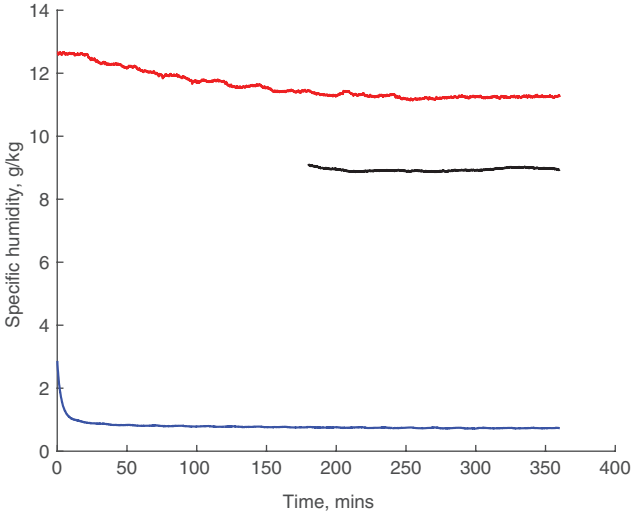

Figure 3: Stabilisation of system after 3 h for both elevated (red) and low (blue) humidity scenarios. Standard condition is indicated in black.

to mean RH levels of 1.69% ± 0.04, 20% ± 1 and 30% ± 1 for low, standard and elevated humidity levels, respectively.

Discussion

Direct write melt electrospinning can be susceptible to variations in processing conditions. Parameters affecting the fabrication process such as polymer temperature, voltage, tip to collector distance and flow rate have been well characterised [4, 19–24]. In this study, a humidity control system allowed changes in humidity levels inside an acrylic chamber completely enclosing the electrospinning apparatus. The humidity system was an open system as opposed to a closed system used by Nezarati et al. [13], where humidity was increased using a humidifier, and decreased using compressed air passing through Drierite™. Maximum and minimum capabilities of the humidity

system was used to investigate changes in scaffold characteristics. Figure 3 shows the humidity levels recorded over approximately 6 h and demonstrated system stability. At approximately 3 h, elevated and low humidity levels plateaued. The maximum achievable humidity of our system due to the temperature differential between the electrospinning enclosure and supply air. The lower temperature in the elevated humidity condition could be attributed to the incoming air being cooled by the saturation chamber. This may have potentially resulted in thicker fibre diameters due to earlier solidification of PCL fibres; however, this was not evident. Higher levels could be achieved in future studies by implementing temperature control of the supply air and/or saturation chamber.

Standard laboratory (standard) humidity level and stability was assessed by supplying only laboratory air into the electrospinning enclosure with humidity recorded over 3 h. Table 1 shows the specific humidity had a mean of 8.94 g/kg ± 0.05. Comparisons between the relative uncertainties of the low, standard and elevated humidity level results, in Table 1, indicated the stability of the laboratory environment, which was comparable to our humidity control apparatus. For consistency, scaffolds were sequentially produced under each humidity level. Although our apparatus did not control the air temperature, it was recorded throughout all fabrication stages with maximum variation of 3%. Pelipenko et al. [7] used a humidity control system which was turned off after the required conditions were met. They observed that during the solution electrospinning process, RH did not change more than 1% with a range studied from 4% to 70%. Similarly, environmental temperature was not controlled in the Pelipenko et al. [7] study. The present study, however, was limited to a maximum RH of 30% as a result of the limited air saturation capabilities of our humidity control hardware. Results of the present study suggest that specific scaffold characteristics such as fibre thickness and fibre surface morphology are not appreciably affected by differences in specific humidity levels of 0.74 g/kg and 11.26 g/kg during fabrication within the characterisation techniques employed. In addition, the present study was limited to structural characteristics and did not consider the potential for humidity to become a factor for more sophisticated biofabrication platforms that combine real-time cell-printing.

Direct write melt electrospun scaffolds are constructed by stacking layers of 2D patterns [25]. For tissue engineering purposes, the ability to obtain a high degree of control is desirable. Specifically when scaffolds are required to contain internal regions of complex multizonal microarchitectures consisting of various pore geometries and micro-channels, which can allow nutrient delivery and metabolic waste removal. Ristovski et al. [1] assessed melt electrospinning precision as a function of scaffold layering with various electric potentials where a quantifiable structure order parameter was introduced. All scaffolds in this study were found to have comparable order parameters, as shown in Table 1. Results suggested that humidity does not appreciably affect the ability to melt electrospin precisely layered 2D patterns, repeatedly. As order parameters were close to 1 (perfect order), this indicated that scaffolds were well ordered at fibre junctions for up to 100 layers. A drawback of this metric is the limited sensitivity to stacking disorder along the line connecting the bottom fibre to the top fibre, which may not be vertically aligned through the layers. This approach is limited to assessment of ordering at fibre junctions only. In addition to this quantitative parameter, 3D μCT reconstruction of the scaffolds did not appear to vary greatly in terms of general scaffold ordering, as shown in Figure 4. These representative images qualitatively indicated that the scaffolds exhibited similar structural characteristics across the three humidity levels.

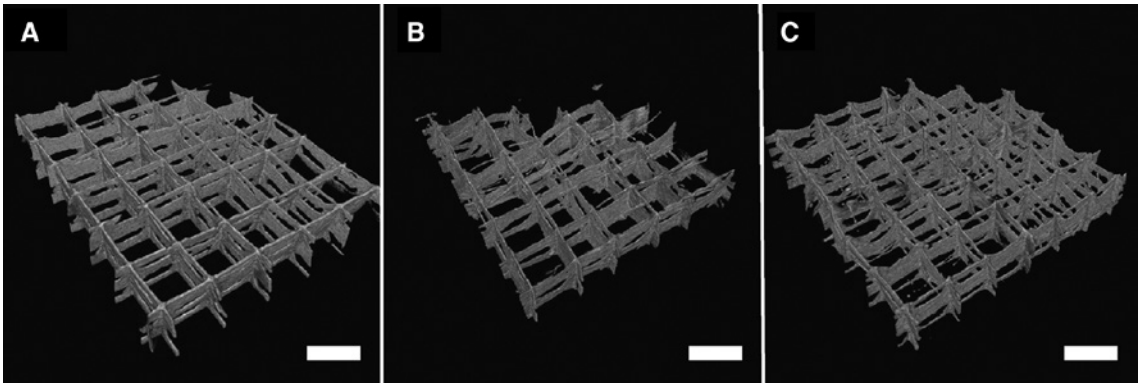

Figure 4: Representative μCT of scaffolds at different humidity levels. (A) Low humidity, (B) standard humidity, (C) elevated humidity. The top-right corner of the scaffolds have been cut off for orientation purposes. Scale bars represent approximately 1 mm.

SEM images of scaffolds in Figure 2 indicate no apparent structural variations between scaffolds produced at the three humidity levels of the present study. No qualitative differences were found with fibre fusion and bridging between the three humidity conditions. Figure 2A, D and G, corroborate the results from the μCT analysis and showed reasonably well-ordered layers. No noticeable difference was found in the surface morphology within the realms of the characterisation technique used, as seen in Figure 2. All images showed characteristic PCL fibre surface morphology with similarly distributed plate boundaries and pit-like features [6]. More detailed surface characterisation techniques potentially capable of detecting variations between the fibres is beyond the scope of the present study. The effect of humidity on scaffold fabrication stability was also supported by the observations of similar average fibre diameters shown in Table 1. Although these results indicate the standard humidity level resulted in fibres with a slightly smaller mean diameter compared to both the elevated and low humidity levels, any significance of this is mitigated by the large statistical variations. In general, the results of this study suggests no significant difference in fibre thickness for scaffolds produced at either low or elevated humidities. This contrasts with the case of the effects of humidity on solution electrospinning, where numerous studies reported significant variations in fibre size and morphology Pelipenko et al. [7]; Ogulata and Icoglu [8]; Bisht et al. [9]; Lu and Xia [10]; Medeiros et al. [11]; Casper et al. [12]; Nezarati et al. [13]. As solution electrospinning relies on solvent evaporation for fibre solidification, the effect of humidity could be expected to be more pronounced compared with melt electrospinning, where fibre solidification is due to polymer cooling.

The results indicated that direct write melt electrospinning of PCL scaffolds with 90° cross-hatch architecture at specific humidity levels between 0.74 g/kg and 11.26 g/kg does not appreciably change the scaffold stacking order, scaffold morphology, fibre surface morphology, and fibre thickness. This has implications for design of melt electrospinning hardware by implying that incorporating complex control over humidity during direct write melt electrospinning may not significantly impact the PCL scaffold fabrication.

Materials and methods

Scaffold production

The scaffolds were produced on our proprietary direct write melt electrospinner, as decribed by Ristovski et al. [1]. PCL (Capa™ 6400, Lot 05011, Perstorp UK Limited) scaffolds were produced with a molten polymer heated to 74 °C and extruded at 45 μL/h using a syringe pump (AL-1000, World Precision Instruments, Sarasota, USA) through a 21 gauge syringe tip. The tip and collector was supplied with +6 kV and –3.2 kV, respectively, separated 10 mm apart.

At each humidity level, low (0.74 g/kg), standard (lab conditions) (8.94 g/kg), and elevated (11.26 g/kg), three square scaffolds (2×2 cm) were produced having 90 degree cross-hatch architecture and adjacent fibre spacings of 1 mm stacked to 100 layers. Stage translation speed was 1000 mm/min. Relative humidity and temperature was logged by a HW4 (ROTRONIC AG, Bassersdorf, Switzerland) sensor. A constant flow of supply air was connected to a solenoid valve (EVT317-5D-02F-Q, SMC, Tokyo, Japan), controlled using an Arduino UNO, switching between a drier (3 kg silica gel, Silica Gel Direct, Stapylton, Australia) and saturator with outlets fed into the electrospinning enclosure. To saturate, air was released from a perforated tube, which was submersed within a water reservoir and the humidified air was captured at the top of the reservoir with an outlet.

Scaffold characterisation

Scanning electron microscopy (SEM): One representative sample from each humidity level was sputtered with gold (Leica EM-SCD005 Sputter Coater, Germany) for 80 s (~100 angstroms). Scaffolds were imaged using a SEM (FEI Quanta 200, The Netherlands). Three different fields of view were taken on each scaffold. Mean fibre diameter was analysed from SEM micrographs in the transverse x–y plane on the 100th (top) layer. ImageJ (V1.48o) was used to measure fibre thickness at 15 random locations. Mean fibre diameter and standard deviation was calculated using IBM SPSS Statistics 23 (IBM Corporation, New York, USA) along with a one-way ANOVA.

MicroCT imaging: Scaffolds were trimmed to fit a 10 mm diameter μCT scanning tube. Scaffolds were cut into four equal sized squares, each with one corner cut to identify orientation. Two of the four samples were randomly selected for μCT scanning (μCT 40, Scanco Medical, Bruettisellen, Switzerland) with 6 μm isotropic voxels. The distance transformation method (DTM) was used to determine the order parameter of the scaffold based on the method described in Ristovski et al. [1]. The 150 μCT slices for each scaffold were loaded into ImageJ and three fibre junctions were identified for measurement. The X, Y and Z coordinates of each of the selected fibre junctions were then measured for each μCT layer. Using the DTM analysis, the junction order parameter was computed for each of the selected junctions. This process was repeated for three scaffolds produced at each humidity level giving a total of 12 unique junctions that were characterised for each of the three humidity levels. Mean order parameter and standard deviation was calculated using IBM SPSS Statistics 23 along with a one-way ANOVA.

Acknowledgments: The authors would like to thank Dr. Roland Steck (Queensland University of Technology) for help with CT and the Australian Postgraduate Awards, Queensland University of Technology, the Institute of Health and Biomedical Innovation and Australian Research Council (LP130100461) for financial support.

Author's statement

Conflict of interest: Authors state no conflict of interest.

Materials and methods

Informed consent: Informed consent not required as no human subjects or specimens were used in this study.

Ethical approval: The research related to human use has been complied with all the relevant national regulations, institutional policies and in accordance the tenets of the Helsinki Declaration, and has been approved by the authors' institutional review board or equivalent committee.

References

1. Ristovski N, Bock N, Liao S, Powell SK, Ren J, Kirby GT, et al. Improved fabrication of melt electrospun tissue engineering scaffolds using direct writing and advanced electric field control. Biointerphases. 2015;10:011006.
2. Tuin SA, Pourdeyhimi B, Loboa EG. Interconnected, microporous hollow fibers for tissue engineering: commercially relevant, industry standard scale-up manufacturing. J Biomed Mater Res A. 2014;102:3311–23.
3. Ahmed FE, Lalia BS, Hashaikeh R. A review on electrospinning for membrane fabrication: Challenges and applications. Desalination. 2015;356:15–30.
4. Dalton PD, Grafahrend D, Klinkhammer K, Klee D, Möller M. Electrospinning of polymer melts: Phenomenological observations. Polymer. 2007;48:6823–33.
5. Pham QP, Sharma U, Mikos AG. Electrospinning of polymeric nanofibers for tissue engineering applications: a review. Tissue Eng. 2006;12:1197–211.
6. Brown TD, Dalton PD, Hutmacher DW. Direct writing by way of melt electrospinning. Adv Mater. 2011;23:5651–7.
7. Pelipenko J, Kristl J, Janković B, Baumgartner S, Kocbek P. The impact of relative humidity during electrospinning on the morphology and mechanical properties of nanofibers. Int J Pharm. 2013;456:125–34.
8. Ogulata RT, Icoglu HI. Interaction between effects of ambient parameters and those of other important parameters on electrospinning of PEI/NMP solution. J Text I. 2015;106:57–66.
9. Bisht G, Nesterenko S, Kulinsky L, Madou M. A computer-controlled near-field electrospinning setup and its graphic user interface for precision patterning of functional nanofibers on 2D and 3D substrates. J Lab Autom. 2012;17:302–8.
10. Lu P, Xia Y. Maneuvering the internal porosity and surface morphology of electrospun polystyrene yarns by controlling the solvent and relative humidity. Langmuir. 2013;29:7070–8.
11. Medeiros ES, Mattoso LH, Offeman RD, Wood DF, Orts WJ. Effect of relative humidity on the morphology of electrospun polymer fibers. Can J Chem. 2008;86:590–9.
12. Casper CL, Stephens JS, Tassi NG, Chase DB, Rabolt JF. Controlling surface morphology of electrospun polystyrene fibers: effect of humidity and molecular weight in the electrospinning process. Macromolecules. 2004;37:573–8.
13. Nezarati RM, Eifert MB, Cosgriff-Hernandez E. Effects of humidity and solution viscosity on electrospun fiber morphology. Tissue Eng Part C: Methods. 2013;19:810–9.
14. Hardick O, Stevens B, Bracewell DG. Nanofibre fabrication in a temperature and humidity controlled environment for improved fibre consistency. J Mater Sci. 2011;46:3890–8.
15. Bock N, Woodruff MA, Hutmacher DW, Dargaville TR. Electrospraying, a reproducible method for production of polymeric microspheres for biomedical applications. Polymers. 2011;3:131–49.
16. Yao S, Wang X, Liu X, Wang R, Deng C, Cuil F, et al. Effects of ambient relative humidity and solvent properties on the electrospinning of pure hyaluronic acid nanofibers. J Nanosci Nanotechnol. 2013;13:4752–8.
17. Detta N, Brown TD, Edin FK, Albrecht K, Chiellini F, Chiellini E, et al. Melt electrospinning of polycaprolactone and its blends with poly(ethylene glycol). Polym Int. 2010;59:1558–62.
18. Tian S, Ogata N, Shimada N, Nakane K, Ogihara T, Yu M. Melt electrospinning from poly(L-lactide) rods coated with poly(ethylene-co-vinyl alcohol). J Appl Polym Sci. 2009;113:1282–8.
19. Kong CS, Jo KJ, Jo NK, Kim HS. Effects of the spin line temperature profile and melt index of poly(propylene) on melt-electrospinning. Polym Eng Sci. 2009;49:391–6.
20. Hutmacher DW, Dalton PD. Melt electrospinning. Chem Asian J. 2011;6:44–56.
21. Lyons J, Li C, Ko F. Melt-electrospinning part I: processing parameters and geometric properties. Polymer. 2004;45:7597–603.
22. Deng R, Liu Y, Ding Y, Xie P, Luo L, Yang W. Melt electrospinning of low-density polyethylene having a low-melt flow index. J Appl Polym Sci. 2009;114:166–75.
23. Ogata N, Yamaguchi S, Shimada N, Lu G, Iwata T, Nakane K, et al. Poly(lactide) nanofibers produced by a melt-electrospinning system with a laser melting device. J Appl Polym Sci. 2007;104:1640–5.
24. Dalton PD, Joergensen NT, Groll J, Moeller M. Patterned melt electrospun substrates for tissue engineering. Biomedical Mater. 2008;3:34109.
25. Hochleitner G, Jüngst T, Brown TD, Hahn K, Moseke C, Jakob F, et al. Additive manufacturing of scaffolds with sub-micron filaments via melt electrospinning writing. Biofabrication. 2015;7:035002.